Stabilization of large silicon fullerenes and related nanostructures through puckering and poly(oligo)merization

Aristides D. Zdetsis
Department of Physics, University of Patras, GR-26500 Patras, Greece
(Received 21 July 2009; revised manuscript received 12 October 2009; published 19 November 2009)

The structure, symmetry, and stability of large Si_nH_n, $n=60$, 70, 76, 80, and 180 cages and the $Si_{60}H_{60}$ ligomers: $Si_{120}H_{116}$, $Si_{180}H_{172}$, and $Si_{240}H_{228}$, together with some related "fullerenes" and nanostructures, are studied by *ab initio* density functional theory and second order Møller-Plesset perturbation theory (for $Si_{60}H_{60}$). It is shown that large cages, $n \geq 60$, can be further stabilized by "puckering" of the Si–Si and Si–H bonds through the endohedral bonding of a number of Si-H pairs without altering the symmetry, in all but the $n=60$ case. For $Si_{60}H_{60}$, the symmetry is slightly reduced from I_h to D_{5d}. Such puckering can also lead to alternative structures of the same symmetry (D_{5d} for $Si_{60}H_{60}$), but not necessarily of the same stability. Alternatively, or in parallel, the "oligomerization" (or polymerization) of the fullerenes can also lead to higher stabilization. The present results seem to suggest that chain (oligo)polymerization is more favorable compared to sidewise polymerization, implying some preference for fullerene-structured silicon nanowires. These results are very promising for the study and possible synthesis of such fullerenes and fullerene-based nanostructures.

DOI: 10.1103/PhysRevB.80.195417 PACS number(s): 61.46.Hk, 61.48.−c, 31.90.+s

I. INTRODUCTION

The discovery of buckminsterfullerene[1] (C_{60}) and other smaller and larger fullerenes, such as C_{20} and C_{70}, stimulated the search for possible similar silicon fullerenes with only marginal or partial success so far. The general methods followed in this search can be classified in three principal categories.[2] The direct approach, seeking structures in full analogy to the carbon fullerenes, the intermediate or mixed approach, which deals with mixed silicon and carbon cages, and the indirect approach, which is the most popular and the most successful.

The main characteristic of calculations based on the direct approach (performed with a variety of theoretical methods) is that, they do not agree with each other (see Ref. 2), although practically all of them agree to nonicosahedral lower symmetry structures, apparently due to the dangling bonds. The higher symmetry distorted Si_{60} structures are the T_h structure obtained by molecular dynamics calculations based on the "full-potential linear-muffin-tin-orbital" (FP-LMTO) method (Li *et al.*),[3] and the C_{2h} puckered ball obtained (among others[2]) by Wang *et al.*[4] using density functional theory. Sheka *et al.*[5] also performed calculations with high spin states and concluded that the Si_{60} ground state is a mixed-spin state nearly degenerate over spins.

As was stated earlier, the indirect method seems to be the most successful and most promising. The cages of the third category, which are usually characterized by high symmetry and relatively large highest occupied molecular orbital–lowest unoccupied molecular orbital (HOMO-LUMO) gaps, can be obtained by two different ways: Those involving endohedral doping with other atoms or groups of atoms, and those involving exohedral doping or coverage with a variety of atoms or molecules. The most popular (and perhaps most successful) of these exohedrally bonded atoms is hydrogen. Yet, the bonding in most of these cages is sp^3 (or near sp^3), not sp^2 as in pure carbon fullerenes.

Hydrogenated cages of varying sizes and symmetries have been considered in rather different contexts by Kumar and Kawazoe,[6] by Zdetsis,[7] and by Karttunen *et al.*[8] Kumar and Kawazoe[6] have considered small hydrogenated cages for $n=8-28$ examining their doping with various metal atoms. Karttunen *et al.*[8] have considered the stability of large icosahedral Si_nH_n "fullerenes" with $n=20$, 60, up to 540, in relation to corresponding polysilanes. Recently, the present author[9] has suggested the connection of Si doped silicon fulleranes (in particular, the $Si_{28}H_{28}$) with the experimentally detected 1 nm luminous Si nanoparticle, thus expanding the idea and scope of hydrogenated silicon cages.

The stability (expressed through the binding energy per Si-H unit) of the silicon "fulleranes" from $n=4$ to $n=60$ varies from 5.06 eV per Si-H unit[6] (for $n=4$) to 6.29 eV per Si-H unit (for $n=60$) reaching its highest value (6.36 eV per Si-H) for $n=20$. Previous experience[10,11] from the corresponding icosahedral carbon fulleranes C_nH_n has shown that the stability of large icosahedral fulleranes ($n \geq 60$) can be improved to values better than $n=20$ by partial endohedral hydrogenation. This allows each H-C-C-H fragment, corresponding to a C-C shared edge, to adopt a chairlike structure with one hydrogen atom pointing inside the cage and one pointing outward,[10,11] leading to a "puckered" cage. This allows for better optimization of the sp^3 bond angles and a resulting energy lowering. Apparently, the same is true for Si_nH_n cages as well.[8] The effect of puckering is more general than just endohydrogenation, which facilitates puckering in the present case. It is well-known for silicon nanotubes[12] and nanowires.[13] A different approach that can better stabilize large cages is by forming $Si_{60}H_{60}$ (or in general Si_nH_n) "oligomers" (dimer, trimer, pentamer, etc.) consisting of two, three, and five (etc.) $Si_{60}H_{60}$ cages joined together in a row. Sheka *et al.*[5] considered plain Si_{60} oligomers in their study of Si_{60}.

In the present investigation, we will consider both approaches (endohedral hydrogenation-puckering, and oligomerization) separately and/or in parallel. In Sec. III, we discuss the results of puckered and nonpuckered fullerenes from $n=60$ up to 180, after a short description of the technical

TABLE I. Binding energy (E_b), HOMO-LUMO gap (H-L), and optical gap (E_g) in eV, together with the symmetry (SYM) of the cages Si_nH_n, characterized by the number n, a label (L) denoting the type of puckering, and/or the number of endohedral hydrogens (see text), as well as figure number (wherever available).

n/L		E_b	H-L	E_g	Symmetry
20		6.356	4.367	5.148	I_h
60	Fig. 1(a)	6.291	4.665	4.359	I_h
60 1	Fig. 1(b)	6.308	4.375	4.000	D_{5d}
60 2	Fig. 1(c)	6.345	4.404	4.081	D_{5d}
70	Fig. 2(a)	6.274	4.461	4.062	D_{5h}
70 1	Fig. 2(b)	6.299	4.177	3.698	D_{5h}
76	Fig. 3(a)	6.264	4.480	3.967	T_d
76 4	Fig. 3(b)	6.305	4.396	3.874	T_d
76 12	Fig. 3(c)	6.355	4.493	3.985	T_d
76 16	Fig. 3(d)	6.347	4.340	3.817	T_d
76 24	Fig. 3(e)	6.281	3.898	3.656	T_d
80	Fig. 4(a)	6.259	4.250	4.238	I_h
80 20	Fig. 4(b)	6.389	3.888	4.290	I_h
180	Fig. 5(a)	6.171	4.124	3.727	I_h
180 60	Fig. 5(b)	6.488	3.924	3.750	I_h
180 120	Fig. 5(c)	6.361	4.239	3.910	I_h

details of the calculations in Sec. II. The puckered and nonpuckered $Si_{60}H_{60}$ oligomers are discussed in Sec. IV. Finally, the conclusions of the present investigation are summarized in Sec. V.

II. SOME TECHNICAL DETAILS OF THE CALCULATIONS

The general theoretical and computational method followed for all clusters and cages is density functional theory (DFT) with the hybrid, nonlocal exchange, and correlation functional of Becke-Lee, Parr, and Yang (B3LYP).[14] These calculations were performed with the TURBOMOL program

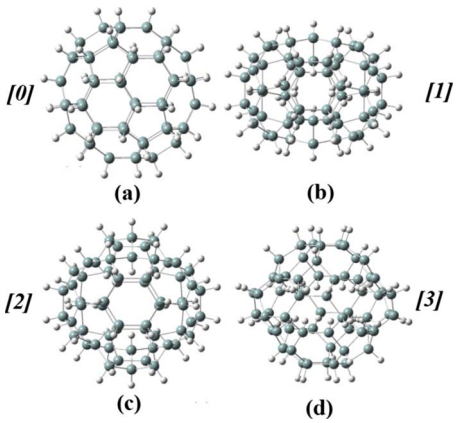

FIG. 1. (Color online) Lowest energy (high symmetry) structures of $Si_{60}H_{60}$. The structure in (a) is the classical icosahedral fullerene (Ref. 6). The puckered structures 1, 2, and 3 in (b), (c), and (d) are characterized by D_{5d} symmetry.

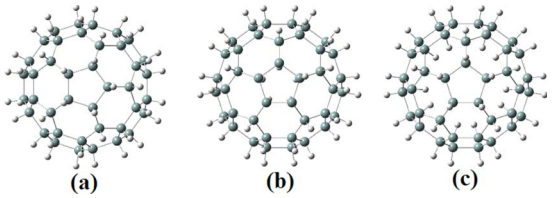

FIG. 2. (Color online) The D_{5h} symmetric lowest energy structures of $Si_{70}H_{70}$ fullerane.

package,[15] using the TZVP basis sets.[16] The same functional (B3LYP) and basis set were used in the time dependent DFT (TDDFT) method for the calculation of the optical gap (excitation gap). For the very large structures, the nonhybrid BP86 functional[15,17] was used employing the "resolution of the identity" (RI) approximation,[15] which greatly improves computational cost. The BP86 functional includes the Becke exchange[17] and the Vosko-Wilk-Nussair[17] (VWN), and Perdew[17] correlation functional. Both B3LYP and BP86 functional were used for several medium size clusters to allow the comparison and extrapolation to large structures. For the lowest energy structures of $Si_{20}H_{20}$ and $Si_{60}H_{60}$, MP2 calculations were performed (starting from the B3LYP/TZVP geometry) with the same basis sets and program package.

III. RESULTS AND DISCUSSION FOR THE Si_nH_n FULLERENES

The results of the present calculations for Si_nH_n fullerenes are summarized in Table I and Figs. 1–5. In Table I, some critical structural, energetic, electronic, and optical characteristics are summarized for $Si_{60}H_{60}$ and the other Si_nH_n single fullerenes examined here. These characteristics include symmetry, binding (atomization) energy, HOMO-LUMO, and optical gap. The binding energy $E_b[Si_nH_n]$ of the Si_nH_n cages is defined (as usual) through the relation $E_b[Si_nH_n]=[E(Si)+E(H)]-E_{tot}/n$, where E(Si), E(H) are the atomic energies of Si and H, respectively, and E_{tot} is the total energy of the Si_nH_n cage. The zero point energy is not included in this definition in order to have a uniform compari-

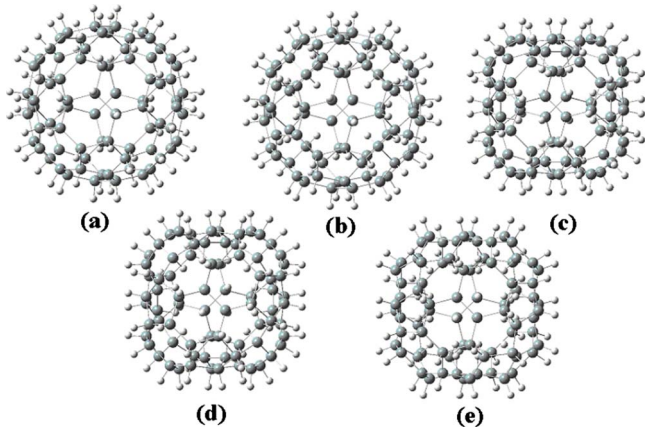

FIG. 3. (Color online) The lowest energy structures of $Si_{76}H_{76}$ fullerene.

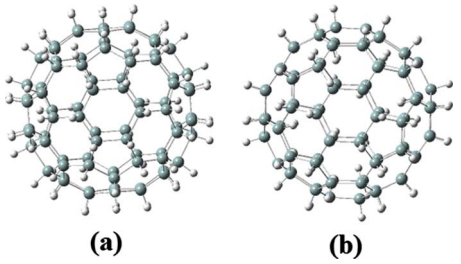

FIG. 4. (Color online) The lowest energy structures of $Si_{80}H_{80}$ icosahedral fullerane. The nonpuckered isomer is shown in (a) and the puckered structure is shown in (b).

son with the larger structures for which frequency calculations are practically impossible due to the large amounts of computer time and space. This does not affect the main results and conclusions of this work. The optical gap is defined here as the excitation energy of the first allowed transition (i.e., with nonzero oscillator strength). Hence, the values quoted in Table I correspond to the lowest singlet excitation with nonzero oscillator strength. In Table I, the characteristic $Si_{20}H_{20}$ fullerene is included as well for comparison, as a reference structure. This fullerene on the basis of binding energy is the most "stable" nonpuckered fullerene, although on the basis of surface curvature or of "kinetic stability" (estimated from the size of the HOMO-LUMO gap)[18] its relative stability compared to $Si_{60}H_{60}$ would be expected to be lower. It is also known that the HOMO-LUMO gap is a zeroth order estimate of the "chemical hardness" of a compound. Yet, the cohesive stability of $Si_{20}H_{20}$ is related with the fact that it consists of only pentagons in which the bond angles are 108°, very close to the ideal sp^3 bond angles of 109.5°. Thus, for the sp^3 optimization, there is no need for any "puckering" and endohedral hydrogenation, as in the case of higher fullerenes containing hexagons (with bond angles of 120°, away from the ideal value. As a result, as we can see in Table I, although the puckered structures 1 and especially 2 are substantially more stable (on the basis of binding energy) than the icosahedral $Si_{60}H_{60}$ isomer, they are still less stable than $Si_{20}H_{20}$ (they have lower values of E_b).

There is an additional strange-looking aspect about $Si_{20}H_{20}$ in Table I: Although the HOMO-LUMO gap is expected to be (and it is, for most structures) larger than the optical gap, for $Si_{20}H_{20}$ exactly the opposite happens, which is related with its high (I_h) symmetry. We can easy understand this if we look closer at the symmetry of the HOMO and LUMO orbitals and the symmetry of the allowed transitions. The HOMO orbital is characterized by h_u symmetry and the LUMO by a_g. This transition is not allowed by symmetry. Due to the high I_h symmetry of $Si_{20}H_{20}$, the only allowed singlet transitions are those of t_{1u} symmetry. The first t_{1u} excitation that determines the optical gap (according to the definition of the optical gap given here) is located at 5.148 eV above the ground state. As a result, the HOMO-LUMO gap cannot be used to estimate the experimental band-gap optical transition. The same effect is also present in several other high-symmetry icosahedral, dodecahedral, and tetrahedral molecules and clusters[19] and also for the icosahedral $Si_{80}H_{80}$ fullerene obtained here (see Table I). In addition, $C_{20}H_{20}$ has a completely similar behavior: its HOMO and LUMO orbitals have the same a_g symmetry with a HOMO-LUMO gap of 7.3 eV, whereas the optical gap has been blueshifted by 2.1 eV. For $Si_{60}H_{60}$, however, although the HOMO (h_u) to LUMO t_{2u} excitation is forbidden, the first allowed t_{1u} transition is only 4.36 eV above the ground state compared to the HOMO-LUMO gap of 4.67 eV. In this case, the optical gap is redshifted by about 0.3 eV. The HOMO-LUMO/optical gap comparison of the $Si_{80}H_{80}$ fullerene are similar to $Si_{20}H_{20}$, whereas fullerene $Si_{180}H_{180}$ is similar to $Si_{60}H_{60}$ in respect to the HOMO-LUMO and optical gap magnitudes.

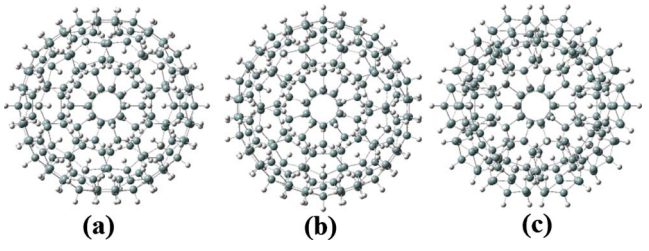

FIG. 5. (Color online) The lowest energy structures of icosahedral $Si_{180}H_{180}$ fullerane with $i=0$ (a), $i=60$ (b), and $i=120$ (c) endohedral hydrogens.

(i) $Si_{60}H_{60}$. The lowest energy (and highest symmetry) structures of $Si_{60}H_{60}$ obtained here are shown in Fig. 1. The structure in Fig. 1(a) is the classical[6] icosahedral structure,[6] whereas the remaining puckered structures in Fig. 1 are characterized by D_{5d} symmetry and 10 (structures b and c) or 20 (structure d) endohedral hydrogens.

The puckered structures, and in particular the structures in Figs. 1(b) and 1(c), have ten endohedral hydrogen atoms in hexagonal chairlike arrangements (with neighboring exohedral hydrogens). Both of these structures are more stable than the icosahedral isomer, with the second puckered structure (structure 2) been the most stable structure in Fig. 1. The high stability of structure 2 in Fig. 1(c), in particular compared to the "similar" structure 1 in Fig. 1(b) characterized by the same D_{5d} symmetry and number (10) of endohedral hydrogens is due to the different type of puckering. In these structures the endohedral hydrogens are bonded to different sets of silicon atoms belonging to different types of silicon rings. In structure 2 in Fig. 1(c) the puckering of hexagonal (and pentagonal) rings is energetically more favorable compared to structure 1 in Fig. 1(b) because the ratio of puckered hexagons to puckered pentagons in this structure (2) is higher compared to the same ratio for the puckered structure 1. As was mentioned above and explained elsewhere[2,8,9] the puckering of hexagons with bond angles far away from the ideal sp^3 bond angles is more favorable compared to pentagons, the bond angles of which are already (before puckering) very close to the ideal sp^3 bond angles. Needless to say that the puckering of the bond angles in hexagons, affects unavoidably also the bond angles of the neighboring pentagons (108°).

Structure 3 in Fig. 1(d), with 20 endohedral hydrogens, is much higher in energy similarly to the corresponding structures of $C_{60}H_{60}$ (see Ref. 11). Another puckered structure with 20 endohedral hydrogens (much higher in energy than

structure 3) is very unstable and becomes disjoint after geometry optimization. This structure (not shown in Fig. 1), which is very similar to a corresponding disjoint structure[11] of $C_{60}H_{60}$, could (after proper manipulation)[11] lead to useful tubular Si structures.[11,12] Structures with 12 or 15 endohedral hydrogens are also higher in energy. It becomes clear, therefore, that similarly to $C_{60}H_{60}$, the number of endohedral hydrogens[11] as well as the type of the Si atoms to which they are attached (type of silicon rings), are very important for the stability of these fullerenes. For $Si_{60}H_{60}$, as for $C_{60}H_{60}$, the "magic" number of endohedral hydrogens is clearly ten.[11]

(ii) $Si_{70}H_{70}$. Even less stable is the $Si_{70}H_{70}$ fullerene in both forms: totally exohedrally [Fig. 2(a)], and partially endohedrally [Figs. 2(b) and 2(c)] hydrogenated fullerenes. The isomer in Fig. 2(c) with 20 endohedral hydrogens is much higher in energy compared to both, the 10 endohedral hydrogens isomer in Fig. 2(b), and the totally exohedral hydrogenated standard fullerene in Fig. 2(a).

Thus, this isomer [in Fig. 2(c)], like the $Si_{60}H_{60}$ isomers in Figs. 1(d) and 1(e), is not included in Table I.

(iii) $Si_{76}H_{76}$. The totally exohedrally hydrogenated silicon fullerene with $n=76$, shown in Fig. 3(a), similarly to C_{76} (and $C_{76}H_{76}$), is T_d symmetric. The T_d symmetry offers more degrees of freedom for partial endohedral hydrogenation. We have examined the cases of $i=4$, 12, 16, and 24 endohedral (76-i exohedral) hydrogens out of 76. The lowest energy structures with $i=4$, 12, 16, and 24 are shown in Figs. 3(b)–3(e), respectively. As we can see in Table I, all these puckered structures have higher binding energies compared to the totally exohydrogenated isomer of Fig. 3(a). The most stable structure is the $i=12$ structure shown in Fig. 3(c), which has practically the same binding energy with $Si_{20}H_{20}$.

In addition, this structure has similar binding energy with $Si_{29}H_{29}$ and the same tetrahedral symmetry.[6] This has led to the conjecture[9] that probably the Si^- or Si embedded form of this fullerene, possibly after the removable of suitable (in number and in type) hydrogens, could be related with the 2.6-nm luminous nanoparticle. The size and symmetry of this $Si_{76}H_{76}$ embedded "fullerane" fit quite well with this conjecture, which, however, will not be pursued here as been beyond the main scope of the present paper.

(iv) $Si_{80}H_{80}$. The C_{80} (and $C_{80}H_{80}$) fullerene and apparently $Si_{80}H_{80}$ is characterized by perfect icosahedral symmetry, similarly to $Si_{20}H_{20}$ and $Si_{60}H_{60}$. However, unlike $Si_{60}H_{60}$ (and $Si_{20}H_{20}$), $Si_{80}H_{80}$ can be partially endohydrogenated without altering its I_h symmetry. The number of such endohedral hydrogens could be either $i=20$, or 60. The $i=60$ puckered isomer is less stable compared to the normal exohydrogenated isomer, probably due to the mutual repulsions between the 60 endohedral hydrogens. The $i=20$ puckered icosahedral $Si_{80}H_{80}$ isomer, however, is substantially more stable than the nonpuckered isomer, as we can see in Table I, exceeding in binding energy even $Si_{20}H_{20}$. This isomer, together with the nonpuckered isomer is shown in Fig. 4.

(v) $Si_{180}H_{180}$ Similarly to $Si_{80}H_{80}$ (and C_{180}), $Si_{180}H_{180}$ is characterized by full I_h symmetry. The efficient number of endohedral hydrogens (i), which preserve icosahedral symmetry in this case, is $i=60$ and 120, shown in Fig. 5. Between the two puckered structures, which both have higher binding energies compared to the $i=0$ standard structure, the $i=60$ isomer in Fig. 5(b) is the most stable with a binding energy of about 6.49 eV. This isomer is by far more stable than both $Si_{20}H_{20}$ and $Si_{80}H_{80}$. The energy difference of 0.132 eV (12.7 kJ/mol) from the reference structure of $Si_{20}H_{20}$ is indeed very large and this isomer seems to be the "champion" in stability from all structures examined in this and other works.[8] The increased stability of $Si_{180}H_{180}$ and other large puckered fullerenes was first recognized by Karttunen *et al.*[8] who illustrated that the stability of even larger cages approaches gradually the stability of polysilanes, although the significance of puckering for Si nanostructures was already known.[12] We can thus see that contrary to the standard nonpuckered silicon fullerenes, the puckered Si_nH_n cages can increase their stability with increasing n, but apparently not uniformly. An alternative way besides puckering that could be also combined with endo-hydrogenation is oligo-, or polymerization, described in the next section (Sec. IV).

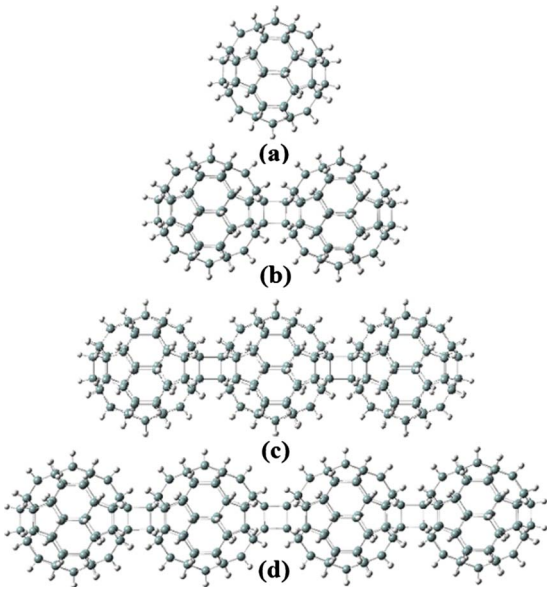

FIG. 6. (Color online) Linear oligomers of $Si_{60}H_{60}$ (see text).

IV. RESULTS AND DISCUSSION FOR FULLERENE OLIGOMERS

The idea of stabilizing Si_{60} through oligomerization in the form of linear chains goes back to Sheka *et al.*,[5] who also considered high spin Si_{60} states. Here, we have examined two, three, and four oligomers of $Si_{60}H_{60}$, both linear (chains) as in Fig. 6, and two-dimensional as in Fig. 7. In both cases, we have considered puckered and nonpuckered structures. Obviously, one could consider oligomers based on $Si_{80}H_{80}$, or even $Si_{180}H_{180}$, or even larger, at (dramatically) increased computational cost. The basic conclusions are expected to be largely the same.

Also, one might be tempted to consider van der Waals interactions between adjacent molecules, which could play a nontrivial role for organic oligomers. If that was the case for the silicon oligomers of Fig. 6 or 7, the DFT approach would

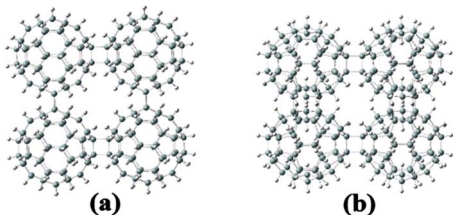

FIG. 7. (Color online) Two-dimensional oligomers of nonpuckered (a) and puckered (b) $Si_{60}H_{60}$ isomers.

be obviously invalid. However, for the present oligomers with such magnitude of cohesive energy, this is clearly not the case and van der Waals interaction, playing no significant role at all, can be safely omitted.

To compare the stability of the various oligomers to each other and to the single fullerenes, we need a different measure of stability than the binding energy, because we need to compare the cohesive stability of various structures with the same number o silicon atoms but different number of hydrogen atoms. Obviously, this is not a problem for the single fullerenes examined in the previous section (same number of Si and H) for which stability differences are equal to binding energy (per Si-H unit) differences. This is mainly due to the different arrangements of the numbers of hydrogens and silicons involved in the various structures. In such cases, as has been illustrated before,[9,11,13] the concept of "cohesive energy" is very useful. The cohesive energy, E_{coh}, which depends on the structure's size, is defined by the relation

$E_{coh}=[\mathrm{BE}(\mathrm{Si}_{N_{\mathrm{Si}}}\mathrm{H}_{N_{\mathrm{H}}})+\mu_{\mathrm{H}}N_{\mathrm{H}}]/N_{\mathrm{Si}}$, where $\mathrm{BE}(\mathrm{Si}_{N_{\mathrm{Si}}}\mathrm{H}_{N_{\mathrm{H}}})$ is the binding (or atomization) energy of the $(\mathrm{Si}_{N_{\mathrm{Si}}}\mathrm{H}_{N_{\mathrm{H}}})$ structure. N_{Si} and N_{H} are the numbers of Si and H atoms, respectively; and μ_{H} is the chemical potential of H, which is taken at a constant value. The constant value of the chemical potential μ_{H} ($\mu_{\mathrm{H}}=-3.46$ eV) is evaluated in such a way so that zero corresponds to the value at which the formation energy of silane (SiH_4) is zero.

This is practically equivalent to effectively removing the energy contribution of all Si–H bonds in every system and essentially considering the binding energy of the "silicon skeleton." For the purpose of the present comparisons and for the fullerene structures examined here, this choice is adequate. To this end, in Table II, we have compiled the cohesive energies of the various oligomers, together with the corresponding values for the $Si_{20}H_{20}$ and $Si_{60}H_{60}$ as reference values. For computer space and time economy, the very large oligomers have been calculated with the nonhybrid BP86 functional using the RI approximation (see Sec. II).

The same method was also used for several "smaller" oligomers in addition to B3LYP for comparison. This, as a by-product of the present work, allows also the comparison of the B3LYP and BP86 results. The present results confirm earlier findings,[20] that BP86 underestimates HOMO-LUMO gaps and overestimate binding. This, however, is not relevant to the subject of the present investigation.

From Table II, we can see that from the single $Si_{60}H_{60}$ fullerene of Fig. 1(a), or of Fig. 6(a), to the corresponding three oligomer of Fig. 6(c) we gain about 0.04 eV per Si-atom (0.036 eV/Si-atom with the B3LYP method or 0.043 eV/Si-atom with the BP86 functional). Although this could be considered as a significant gain, we are still behind the $Si_{20}H_{20}$ stability by about 0.02 eV per Si-atom (0.029 with B3LYP). Only with the fourth linear oligomer in Fig. 6(d) we can surpass the stability of $Si_{20}H_{20}$ by about the same amount (0.022 eV per Si atom) without puckering. By puckering, we can accomplish the same gain with the double puckered oligomer. This suggests that puckering is more efficient than oligomerization. This is also verified by comparing the gain from double oligomerization of $Si_{60}H_{60}$ (0.027 eV/Si-atom, at the B3LYP level) with the gain from puckering (0.054 eV/Si-atom, at the B3LYP level), which is double. Yet, the difference in stability (cohesive energy gain) between the stability of single $Si_{60}H_{60}$ fullerene and double oligomer is practically the same (0.029 and 0.027 eV/Si-atom, respectively) for both puckered and nonpuckered structures, which seems to imply that oligomerization has practically the same influence in puckered and nonpuckered fullerenes. This is also suggested by the almost constant cohesive energy differences between puckered and nonpuckered structures, which are: 0.054 eV/Si-atom for the single fullerene; 0.056 eV/Si-atom for the double oligomer; and 0.050 eV/Si-atom (at the BP86 level) for the four sidewise (two-dimensional) oligomer. It is also clear from Table II that sideways oligomerization is less efficient compared to linear oligomerization (at least for nonpuckered fullerenes). This could be very important for fullerene-structured silicon nanowires.[21]

TABLE II. Cohesive energy (E_{coh}), and HOMO-LUMO gap in eV, together with the symmetry (SYM) of the $Si_{60}H_{60}$ oligomers, characterized by the number N of Si atoms and a label (L) denoting the number and type of oligomers (see text). $Si_{20}H_{20}$ and $Si_{60}H_{60}$ are listed for comparison. Energies calculated with the BP86 functional are shown in italics at the second entry of each row.

n/L		E_{coh}	H-L	Symmetry
20		2.897	4.367	I_h
		3.105	*3.152*	
60	Fig. 6(a)	2.832	4.665	I_h
		3.042	*3.419*	
120 2×	Fig. 6(b)	2.859	4.029	D_{2h}
		3.074	*2.873*	
120 2×1		2.876	3.868	C_{2h}
120 2×2		2.915	3.968	C_{2h}
180 3×	Fig. 6(c)	2.868	3.990	C_{2h}
		3.085	*2.829*	
240 4× linear				C_{2h}
	Fig. 6(d)	*3.127*	*2.814*	
240 2×2 sideways				D_{2h}
	Fig. 7(a)	*3.106*	*2.793*	
240 2×2× sideways 2				C_{2h}
	Fig. 7(b)	*3.156*	*2.666*	

V. CONCLUSIONS

It has been illustrated that there are two important mechanisms to better stabilize large Si_nH_n cages: puckering and/or oligo- or polymerization. Puckering, which is also important for nanotubes and nanowires,[12,13] is more efficient than oligomerization. The combined effect of the two can give very stable fullerenes or chains of fullerenes. Obviously, concerning oligo-polymerization we could have had better overall results by considering $Si_{20}H_{20}$ or, even better, puckered $Si_{80}H_{80}$ (preferably linear), or best of all, $Si_{180}H_{180}$ oligomers.

Larger oligomers are more stable than smaller ones or than single fullerenes. However, the difference in energy gain between successive oligomers is decreasing with increasing size, apparently approaching some constant limiting value for very large oligomers (polymers).

Similar results more or less hold for the energy gain by puckering as the fullerene size increases up to $Si_{180}H_{180}$, which seems to be an optimal case.

The present results seem to suggest that chain (oligo)polymerization is energetically more favorable compared to sidewise polymerization, implying some preference for fullerene-structured silicon nanowires and/or nanotubes. These results are very promising for the study and possible synthesis of such fullerenes and fullerene-based nanostructures.

[1] H. W. Kroto, J. R. Heath, S. C. O'Brien, R. F. Curl, and R. E. Smalley, Nature (London) **318**, 162 (1985).

[2] A. D. Zdetsis, in *Handbook of Nanophysics*, edited by K. D. Sattler (Taylor & Francis, London, in press).

[3] Bao-xing Li, Pei-lin Cao, and Duan-lin Que, Phys. Rev. B **61**, 1685 (2000).

[4] L. Wang, D. Li, and D. Yang, Mol. Simul. **32**, 663 (2006).

[5] E. F. Sheka, E. A. Nikitina, V. A. Zayets, and I. Y. Ginzburg, Int. J. Quantum Chem. **88**, 441 (2002).

[6] A. D. Zdetsis, Phys. Rev. B **76**, 075402 (2007); **75**, 085409 (2007).

[7] V. Kumar and Y. Kawazoe, Phys. Rev. B **75**, 155425 (2007); Phys. Rev. Lett. **90**, 055502 (2003).

[8] A. J. Karttunen, M. Linnolahti, and T. A. Pakkanen, J. Phys. Chem. C **111**, 2545 (2007).

[9] A. D. Zdetsis, Phys. Rev. B **79**, 195437 (2009).

[10] M. Linnolahti, A. J. Karttunen, and T. A. Pakkanen, ChemPhysChem **7**, 1661 (2006).

[11] A. D. Zdetsis, Phys. Rev. B **77**, 115402 (2008).

[12] G. Seifert, Th. Köhler, H. M. Urbassek, E. Hernández, and Th. Frauenheim, Phys. Rev. B **63**, 193409 (2001).

[13] A. D. Zdetsis, E. N. Koukaras, and C. S. Garoufalis, Appl. Phys. Lett. **91**, 203112 (2007).

[14] P. J. Stephens, F. J. Devlin, C. F. Chabalowski, and M. J. Frisch, J. Phys. Chem. **98**, 11623 (1994).

[15] TURBOMOLE, Version 5.6 (Universitat Karlsruhe, 2000).

[16] A. Schäfer, C. Huber, and R. Ahlrichs, J. Chem. Phys. **100**, 5829 (1994).

[17] A. D. Becke, Phys. Rev. A **38**, 3098 (1988); S. H. Vosko, L. Wilk, and M. Nusair, Can. J. Phys. **58**, 1200 (1980); J. P. Perdew, Phys. Rev. B **33**, 8822 (1986).

[18] D. E. Manolopoulos, J. C. May, and S. E. Down, Chem. Phys. Lett. **181**, 105 (1991).

[19] R.-H. Xie, G. W. Bryant, J. Zhao, T. Kar, and V. H. Smith, Jr., Phys. Rev. B **71**, 125422 (2005).

[20] C. S. Garoufalis, A. D. Zdetsis, and S. Grimme, Phys. Rev. Lett. **87**, 276402 (2001); A. D. Zdetsis, C. S. Garoufalis, and S. Grimme, in *Quantum Dots: Fundamentals, Applications, and Frontiers (Crete 2003)*, edited by B. A. Joyce *et al.*, NATO Science Series, Vol. 190 Series II, Mathematics, Physics, and Chemistry (Kluwer-Springer, Dordrecht, The Netherlands, 2005), pp. 317–332.

[21] B. Marsen and K. Sattler, Phys. Rev. B **60**, 11593 (1999).